

## Preparation and characterization of $\text{ZrO}_2\text{-Al}_2\text{O}_3$ particulate nanocomposites produced by plasma technique

Janis Grabis, Ints Steins, Dzintra Rasmane, Aija Krumina  
and Maris Berzins

Institute of Inorganic Chemistry, Riga Technical University, 34 Miera str., Salaspils-1, LV 2169, Latvia; grabis@nki.lv

Received 2 June 2006, in revised form 14 September 2006

**Abstract.** Nanosized spherical  $\text{ZrO}_2(\text{Y}_2\text{O}_3)\text{-Al}_2\text{O}_3$  particulate composites with average particle size in the range of 30–40 nm have been prepared by evaporation of coarse grained oxides in an inductively coupled plasma. The powders contain m-, t- $\text{ZrO}_2$  and  $\theta$ -,  $\delta$ - $\text{Al}_2\text{O}_3$  phases. The presence of  $\text{Al}_2\text{O}_3$  reduces the crystallite size of  $\text{ZrO}_2$  and increases the content of the t- $\text{ZrO}_2$  phase and prevents phase transition of  $\text{ZrO}_2$  during additional calcinations. The surface characteristics of  $\text{ZrO}_2\text{-Al}_2\text{O}_3$  particles testify that zirconia particles are covered by alumina.

**Key words:** nanosized zirconia-alumina, plasma technique, phase composition, particle, crystallite size.

### 1. INTRODUCTION

Zirconia-alumina composites find wide application as high-temperature materials in cutting tools, ball bearings and furnace materials due to their high melting point, mechanical properties, fracture toughness, corrosion and shock resistance [<sup>1,2</sup>]. At present zirconia-alumina composites are commercially available, but materials produced from such composites show poor microstructural homogeneity, particularly with respect to the grain size and phase distribution [<sup>3</sup>]. A promising approach to the improvement of the microstructure and homogeneity of the composite material is application of homogeneous nanosized  $\text{ZrO}_2\text{-Al}_2\text{O}_3$  powders and their fast sintering [<sup>4,5</sup>]. To obtain the finest grain size and possibly high homogeneity of components, several methods of preparation of nanosized powders have been developed [<sup>6,7</sup>]. The  $\text{ZrO}_2\text{-Al}_2\text{O}_3$  powders have

been prepared by the hydrolysis of zirconium propoxide in a dispersion of  $\alpha$ -alumina particles in ethanol [8] by simultaneous hydrolysis of zirconium and aluminium isopropoxides [9], by controlled hydrolysis of chlorides [10] or by a hydrothermal process [4]. Nanosized  $\text{ZrO}_2\text{-Al}_2\text{O}_3$  particulate composites with uniform distribution of components have been obtained by these methods. However, the wet chemical methods of synthesis of  $\text{ZrO}_2\text{-Al}_2\text{O}_3$  powders include many stages and the used raw materials are usually expensive. Besides this, the production rates are relatively low.

Another approach is connected with the synthesis of nanosized powders from the vapour phase by using laser evaporation [11] or the thermal plasma technique [7]. The laser evaporation technique provides preparation of nanosized powders with narrow particle size distribution, but production rate is low in comparison with the plasma technique.

The aim of the present work is to develop a single-step plasma technique for producing highly homogeneous zirconia-alumina particulate composites and to study their characteristics.

## 2. EXPERIMENTAL

The thermal plasma technique is based on the evaporation of coarse-grained commercially available powders in inductively coupled air plasma using the technological equipment described in [12]. The zirconia and alumina powders with a particle size in the range of 10–30  $\mu\text{m}$  are mixed and injected into the plasma flame by the carrier gas. Evaporation of raw oxides is achieved by varying the power of the RF oscillator, the flow rate of the plasma forming gas, feeding rate of the powder and their injection velocity. The formation of particles from vapours and their growth are controlled by introducing cold air into the reaction chamber.

Chemical and phase composition of the prepared oxides are determined by conventional chemical and X-ray diffraction analysis. The specific surface area is determined by argon adsorption-desorption method and the average particle size is calculated from these data. The crystallite size of zirconia phases is determined by the X-ray line broadening method using the Scherrer equation. The particle size and surface morphology are studied by scanning electronic microscopy (SEM) and X-ray microanalysis (EDX). The particle size distribution is studied by the photon correlation spectroscopy method and the surface characteristics of prepared particles are determined by electrokinetic titration of powder suspensions using a computer-controlled system, which combines Zetamaster S of Malvern Instruments Ltd., Mettler DL 21 autotitrator and ultrasonic equipment.

### 3. RESULTS AND DISCUSSION

The formation of particles from vaporous phase results in obtaining homogeneous nanosized powders the characteristics of which depend on the ratio of components. The typical characteristics of prepared in similar conditions nanosized powders in the  $\text{ZrO}_2(\text{Y}_2\text{O}_3)\text{-Al}_2\text{O}_3$  system are shown in Table 1.

The specific surface area of the produced powders is in the range of 29–46  $\text{m}^2/\text{g}$  and increases with the content of alumina mainly due to the change of the specific weight of particles. Weaker dependence of the average particle size on the content of alumina is caused by the decrease of the specific weight of the particles.

The qualitative phase composition of powders is similar but quantitative phase composition depends on the content of alumina and yttria. There is a clear tendency of decrease of the m- $\text{ZrO}_2$  phase with the increase of  $\text{Al}_2\text{O}_3$  content. This indicates that alumina promotes stabilization of zirconia. However, full stabilization of high temperature phases of zirconia was not achieved even at high content of alumina. The crystallite sizes of m- and t- $\text{ZrO}_2$  phases also decrease with the increase of  $\text{Al}_2\text{O}_3$  (Fig. 1).

The data testify that combining synthesis of zirconia and alumina from vapour phase reduces crystallite size of both zirconia phases and content of m- $\text{ZrO}_2$  in prepared powders with respect to pure nanosized  $\text{ZrO}_2$ . The crystallite size of t- $\text{ZrO}_2$  phase is in the range of 20–30 nm and the content of m- $\text{ZrO}_2$  phase is in the range of 8–16% if the powders contain more than 40 wt% of alumina. This shows that the stabilization of t- $\text{ZrO}_2$  phase can be achieved by the so-called size effect. Besides this, the high amount of t- $\text{ZrO}_2$  phase in the powders with low content of alumina and crystallite size above 30 nm indicate the dissolution of

**Table 1.** Characteristics of produced  $\text{ZrO}_2(\text{Y}_2\text{O}_3)\text{-Al}_2\text{O}_3$  samples

No.	Chemical composition, wt%			SSA, $\text{m}^2/\text{g}$	<i>d</i> , nm	XRD
	$\text{ZrO}_2$	$\text{Al}_2\text{O}_3$	$\text{Y}_2\text{O}_3$			
1	99.8	–	–	29.3	34.8	t-, m- $\text{ZrO}_2$ (33%)
2	80.4	19.4	–	37.0	30.0	t-, m- $\text{ZrO}_2$ (20%)
3	70.5	29.4	–	39.5	29.2	t-, m- $\text{ZrO}_2$ (18%) $\theta$ -, $\delta$ - $\text{Al}_2\text{O}_3$
4	51.0	48.8	–	38.3	33.0	t-, m- $\text{ZrO}_2$ (16%) $\theta$ -, $\delta$ - $\text{Al}_2\text{O}_3$
5	24.0	75.9	–	41.4	35.0	t-, m- $\text{ZrO}_2$ (15%) $\theta$ -, $\delta$ - $\text{Al}_2\text{O}_3$
6	14.3	85.5	–	46.3	39.4	t-, m- $\text{ZrO}_2$ (15%) $\theta$ -, $\delta$ - $\text{Al}_2\text{O}_3$
7	85.1	22.2	2.5	34.9	31.8	t-, m- $\text{ZrO}_2$ (10%) $\theta$ -, $\delta$ - $\text{Al}_2\text{O}_3$
8	19.0	80.0	0.8	46.3	32.0	t-, m- $\text{ZrO}_2$ (8%) $\theta$ -, $\delta$ - $\text{Al}_2\text{O}_3$
9	–	99.8	–	44.1	37.0	$\theta$ -, $\delta$ - $\text{Al}_2\text{O}_3$

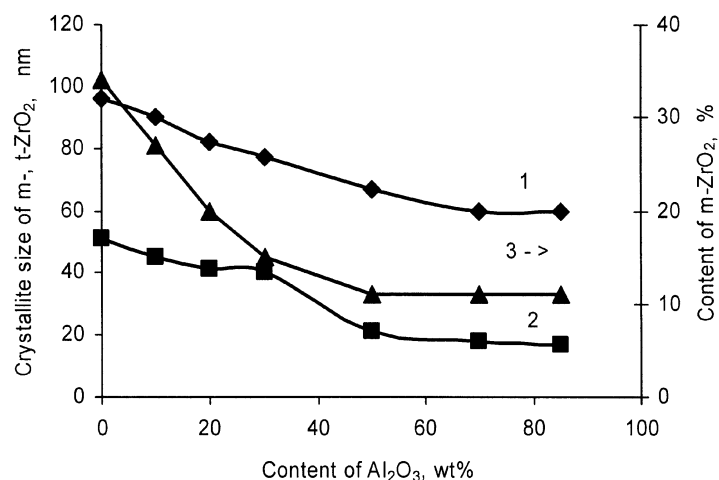


**Fig. 1.** Dependence of the crystallite size of m-ZrO<sub>2</sub> (1) and t-ZrO<sub>2</sub> (2) phases and of the content of m-ZrO<sub>2</sub> (3) in ZrO<sub>2</sub>-Al<sub>2</sub>O<sub>3</sub> powders on the content of Al<sub>2</sub>O<sub>3</sub>.

alumina in zirconia. ZrO<sub>2</sub>-Al<sub>2</sub>O<sub>3</sub> solid solution formation has been obtained during the hydrolysis of zirconium and aluminium izopropoxides [9].

The determined particle size distribution of ZrO<sub>2</sub>-Al<sub>2</sub>O<sub>3</sub> is practically independent of the content of alumina (Fig. 2). Contrary to the calculated data of average particle size, the particle size distribution curves show that mean particle size is around 100 nm and the size of certain particles reaches 300–800 nm.

Differences in values of the particle size can be explained by SEM studies. SEM images and X-ray microanalysis show that the produced ZrO<sub>2</sub>-Al<sub>2</sub>O<sub>3</sub> particles are highly agglomerated and form a fibrous structure (Fig. 3). However, SEM images at high magnification show that fibrous structure consists of spherical particles with size in the range of 20–60 nm (Fig. 4). Therefore different values of average particle size can be caused by the formation of agglomerated particles.

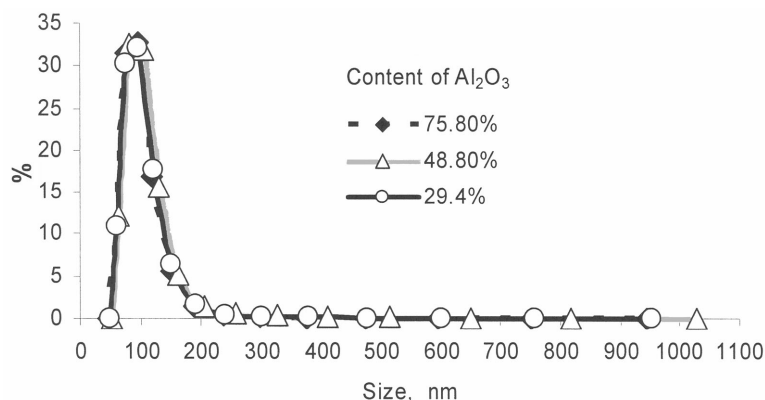


**Fig. 2.** Size distribution of ZrO<sub>2</sub>-Al<sub>2</sub>O<sub>3</sub> particles.

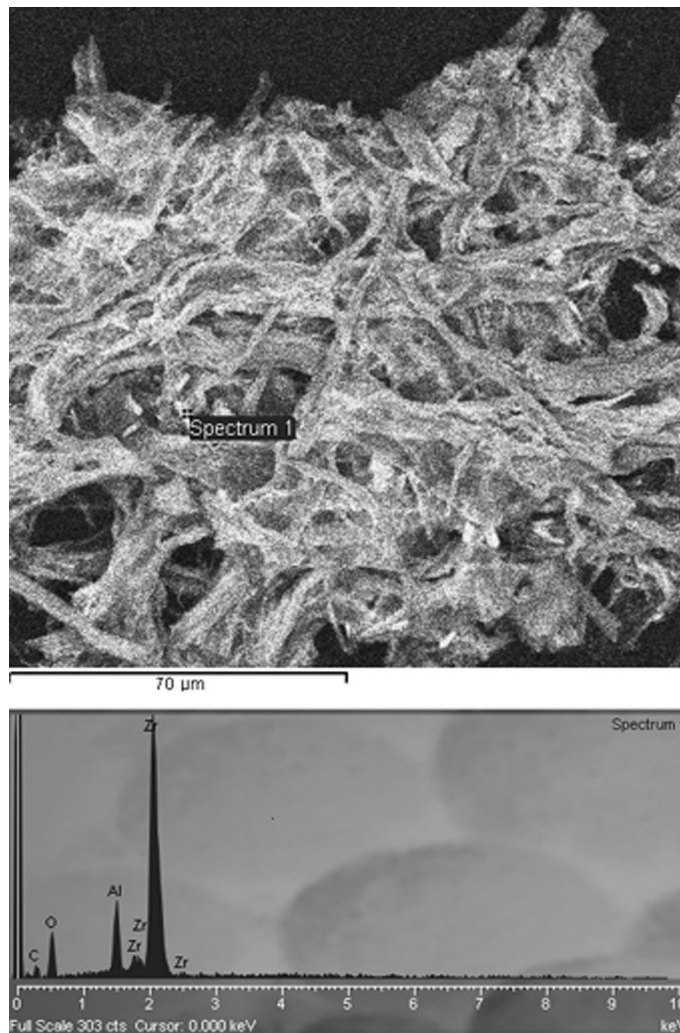


**Fig. 3.** SEM micrographs of  $\text{ZrO}_2\text{-Al}_2\text{O}_3$  particles at low magnification and EDX spectra.

The relatively high crystallite size compared to average particle size can be explained by the presence of separate coarse particles. Such wide particle size distribution is characteristic for powders of refractory compounds, produced by thermal plasma technique, and is connected with different growth conditions of particles due to high temperature and velocity gradients of the plasma flow as well as to collisions of liquid particles or uncomplete evaporation of raw particles.

Additional calcination of  $\text{ZrO}_2\text{-Al}_2\text{O}_3$  powders decreases the specific surface area and average particle size at the temperature above  $900^\circ\text{C}$ . Simultaneously calcination influences the crystallite size of zirconia and phase composition of powders (Fig. 5).

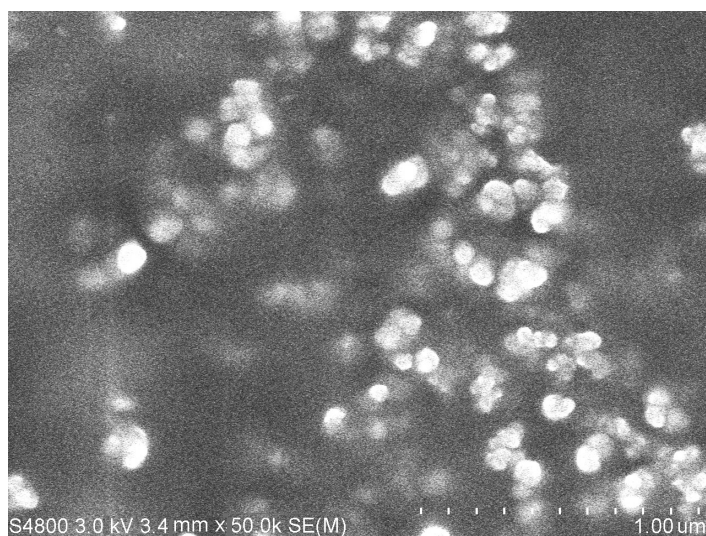


**Fig. 4.** SEM micrographs of  $ZrO_2-Al_2O_3$  particles at high magnification.

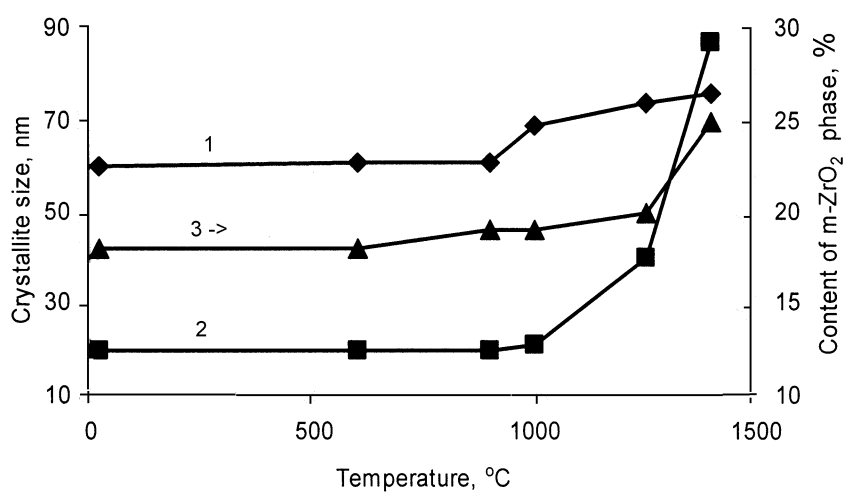


**Fig. 5.** Dependence of the crystallite size of m-ZrO<sub>2</sub> (1) and t-ZrO<sub>2</sub> (2) phases and content of the m-ZrO<sub>2</sub> (3) phase of  $ZrO_2-Al_2O_3$  (78.9 wt%) on the calcination temperature.

The growth of crystallites of both zirconia phases starts at 900°C. Obviously the higher growth rate of t-ZrO<sub>2</sub> phase crystallites compared to m-ZrO<sub>2</sub> phase crystallites is connected with high content of the tetragonal phase. Despite the growing crystallite size at high temperature, the increase of the content of the m-ZrO<sub>2</sub> phase is insignificant. At the temperature of 1400°C the crystallite size of m-ZrO<sub>2</sub> and t-ZrO<sub>2</sub> phases is 78 nm and 85 nm, respectively, but the content of m-ZrO<sub>2</sub> reaches only 25%.

At similar calcination conditions, the growth of the crystallite size of pure zirconia phases starts at 500–550°C and at 1000°C the crystallite size of t-ZrO<sub>2</sub> and m-ZrO<sub>2</sub> reaches 54 nm and 86 nm, respectively. The growth of the crystallite size causes the phase transition of tetragonal modification of zirconia to monoclinic and content of the latter reaches 100% at 1200°C. Therefore the results testify that the presence of Al<sub>2</sub>O<sub>3</sub> eliminates the growth of the crystallite size at the temperature up to 900°C and it stabilizes the zirconia tetragonal phase.

This feature of ZrO<sub>2</sub>-Al<sub>2</sub>O<sub>3</sub> particulate nanocomposites can be explained partially by the particle surface characteristics by electrokinetic titration (Fig. 6).

Analysis of the titration curves shows that the surface of ZrO<sub>2</sub> in the presence of alumina is transformed. The titration curves of ZrO<sub>2</sub>-Al<sub>2</sub>O<sub>3</sub> particles are shifted to the side of higher pH relative to pure ZrO<sub>2</sub> and they are close to the titration curve of Al<sub>2</sub>O<sub>3</sub>.

Similarity of the titration curves of ZrO<sub>2</sub>-Al<sub>2</sub>O<sub>3</sub> and Al<sub>2</sub>O<sub>3</sub> samples indicates that surface characteristics of ZrO<sub>2</sub>-Al<sub>2</sub>O<sub>3</sub> particles are similar to those of alumina. This allows to suppose that the surface of zirconia is at least partially covered with alumina. Formation of such particles from the vapour phase is connected with different boiling temperatures of the compounds. The zirconia particles, formed at higher temperature, can act as nuclei for the deposition of alumina. The complex microstructure of the prepared ZrO<sub>2</sub>-Al<sub>2</sub>O<sub>3</sub> particles limits contacts between ZrO<sub>2</sub> particles and therefore hinders crystallite growth during calcination.

On the other hand, the high content of t-ZrO<sub>2</sub> phase at 1400°C and crystallite size of t-ZrO<sub>2</sub> phase (85 nm) indicate that stabilization of the high-temperature modification of zirconia partially can be related to the formation of the solid solution of Al<sub>2</sub>O<sub>3</sub> in ZrO<sub>2</sub>.

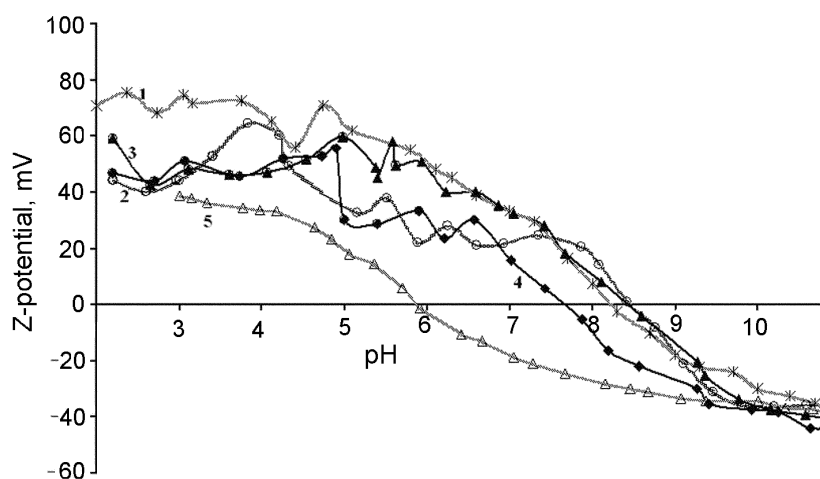


**Fig. 6.** Z-potential curves: 1 – ZrO<sub>2</sub>/75.9% Al<sub>2</sub>O<sub>3</sub>; 2 – ZrO<sub>2</sub>/48.8% Al<sub>2</sub>O<sub>3</sub>; 3 – ZrO<sub>2</sub>/29.4% Al<sub>2</sub>O<sub>3</sub>; 4 – δ-, θ-Al<sub>2</sub>O<sub>3</sub>; 5 – t-, m-ZrO<sub>2</sub>.

#### 4. CONCLUSIONS

1. The developed thermal plasma technique allows to prepare spherical nano-sized  $\text{ZrO}_2\text{-Al}_2\text{O}_3$  particulate nanocomposites with average particle size in the range of 30–40 nm, containing m-, t- $\text{ZrO}_2$  and  $\theta$ -,  $\delta$ - $\text{Al}_2\text{O}_3$  phases.
2. The presence of alumina reduces the crystallite size of zirconia phases and increases the content of the t- $\text{ZrO}_2$  phase relative to pure  $\text{ZrO}_2$ , prepared in similar conditions.
3. Alumina prevents the growth of the crystallite size and phase transition t $\rightarrow$ m- $\text{ZrO}_2$  during calcination at high temperature.
4. The electrokinetic titration curves testify that zirconia particles are covered with alumina.

#### ACKNOWLEDGEMENT

We thank Dr. A. Patmalnieks from Latvian University for SEM studies and X-ray microanalysis of the samples.

#### REFERENCES

1. Biswas, N. C. and Chaudhuri, S. P. Effect of thermal-shock and autoclave treatment on the microstructure of  $\text{Al}_2\text{O}_3\text{-ZrO}_2$  composites. *Ceram. Int.*, 1997, **23**, 69–72.
2. Hisamori, N. and Kimura, Y. Correlation between microstructure and strength characteristics of  $\text{ZrO}_2$ -particle-dispersed  $\text{Al}_2\text{O}_3$ . *Nippon Kikai Gakkai Ronbunshu, A-hen*, 1996, **62**, 908–914.
3. Kerwijk-Mulder, E. and Verweij, H. Zirconia-alumina ceramic composites with extremely high wear resistance. *Adv. Ceram. Mat.*, 1999, **1**, 69–71.
4. Mills, H. and Blackburn, S. Zirconia toughened aluminas by hydro-thermal processing. *J. Eur. Ceram. Soc.*, 2000, **20**, 1085–1090.
5. Jayaseelan, D. D., Kondo, N., Rani, D. A., Ueno, S., Ohji, T. and Kanzaki, S. Pulse electric current sintering of  $\text{Al}_2\text{O}_3/3$  vol.%  $\text{ZrO}_2$  with constrained grains and high strength. *J. Amer. Ceram. Soc.*, 2002, **85**, 2870–2872.
6. Crushing, B. L., Kolesnichenko, V. L. and O'Connor, C. J. Recent advances in the liquid-phase synthesis of inorganic nanoparticles. *Chem. Rev.*, 2004, **104**, 3885–3945.
7. Kong, P. C. and Lau, Y. C. Plasma synthesis of ceramic powders. *Pure Appl. Chem.*, 1990, **62**, 1809–1816.
8. Fegley, B. Jr., White, P. and Brown, H. K. Preparation of zirconia-alumina powders by zirconium alkoxide hydrolysis. *J. Amer. Ceram. Soc.*, 1985, **68**, C60–C62.
9. Yamaguchi, O., Shirai, M. and Yoskinaka, M. Formation and transformation of cubic  $\text{ZrO}_2$  solid solution in the system  $\text{ZrO}_2\text{-Al}_2\text{O}_3$ . *J. Amer. Ceram. Soc.*, 1988, **71**, C510–C512.
10. Mondal, A. and Ram, S.  $\text{Al}^{+3}$ -stabilized c- $\text{ZrO}_2$  nanoparticles at low temperature by forced hydrolysis of dispersed metal cations in water. *Solid State Ionics*, 2003, **160**, 69–181.
11. Popp, U., Herbig, R., Michel, G., Mueller, E. and Oestrich, Ch. Properties of nanocrystalline ceramic powders prepared by laser evaporation and recondensation. *J. Eur. Ceram. Soc.*, 1998, **18**, 1153–1160.
12. Grabis, J., Kuzjukevics, A., Rasmane, D., Morgensen, M. and Linderoth, S. Preparation of nanocrystalline YSZ powders by plasma technique. *J. Mater. Sci.*, 1998, **33**, 723–728.

## **Plasmatehnoloogia abil toodetud $ZrO_2-Al_2O_3$ osakekestest nanokomposiidid**

Janis Grabis, Ints Steins, Dzintra Rasmāne, Aija Krumina ja Maris Berzins

Jāmedateraliste oksiidide aurustamise teel plasmajoas on valmistatud nanosuuruselga (30–40 nm) sfāirilistest  $ZrO_2(Y_2O_3)-Al_2O_3$  osakekestest nanokomposiidid. Āsja valmistatud pulber sisaldab m-, t- $ZrO_2$  ja  $\theta$ -,  $\delta$ - $Al_2O_3$  faase. On nāidatud, et  $Al_2O_3$  olemasolu vāhendab  $ZrO_2$  kristallide suurust ning suurendab t- $ZrO_2$  faasi sisaldust ja takistab  $ZrO_2$  faaside muutumist tēiendaval kuumutamisel.  $ZrO_2-Al_2O_3$  osakeste pinna uurimine kinnitab, et  $ZrO_2$  osakeste pind on kaetud  $Al_2O_3$  kihiga.